Neural Network for Fretting Wear Modeling

Laura HAVIEZ[1a&b,2], Rosario TOSCANO[1b], Siegfried FOURVY[1a] and Ghislain YANTIO[2]

1 LTDS, UMR 5513, (a) Ecole Centrale de Lyon, Ecully, France; (b) ENISE, Saint-Etienne, France.
2 SAGEM, Boulogne-Billancourt Cedex, France.
laura.haviez@ec-lyon.fr, rosario.toscano@enise.fr, siegfried.fouvry@ec-lyon.fr, ghislain.yantio@sagem.com

Abstract: Materials wear is a very complex, only partially-formalized phenomenon involving numerous parameters and damage mechanisms. The need to characterize wear in many industrial applications prompted the present research. The study concerns an original strategy investigating the effect of contact conditions on the wear behavior of carburized stainless steels under fretting and reciprocating sliding motion. A physical model was constructed, and pre-treated experimental data were incorporated in a neural network to model wear volume. Three models are proposed and compared, according to input.

1   INTRODUCTION

Wear is generally defined as loss of surface material from contact surfaces subjected to relative motion. Tribologic issue must therefore be taken into consideration, and several models have been developed in recent years (Kolodziejczyk, 2010; Zhang, 2003). These models usually correlate wear volume with physical and geometrical quantities such as load, sliding distance, coefficient of friction, hardness, materials (Anand Kumar, 2013; Genel, 2003; Sahraoui, 2004), and physical laws such as the Archard wear criterion (Archard, 1953). Many parameters influence wear. To identify one relevant parameter, we chose a neural network to model wear, creating an experimental database: the great advantage of Artificial Neural Networks (ANNs) is their ability to be used as an arbitrary function approximation mechanism which 'learns' from observed data. Fretting damage was used as a case study. Small oscillatory movements may induce interface fretting, shortening predicted lifetime. The interface wear response was modeled and empirical models were created based on data from fretting tests. The Artificial Intelligence model was validated against the physical description of fretting wear behavior.

2   EXPERIMENTAL PROCEDURE

2.1   Material and Contact Type

Tests were performed on two chromium-molybdenum stainless steels: one carburized stainless steel (M1) and one stainless steel with mass quenching (M2). The M1 specimen comprised 3 layers: the external layer was hard and decarburized layer (white layer: WL); the second was the carburized phase (CL), with hardness gradient between 760 HV and 550HV (Figure 1a); the third was the bulk, with 500 HV hardness. These materials were studied to determine the wear kinetics of a two cross-cylinder configuration. According to Hertz, this configuration is equivalent to a sphere/plane configuration where M1 is mobile and M2 fixed. The two cylinders had the same radius (7.5 mm) and the same length (20 mm). The normal force was adjusted to reach 2,200 MPa Hertzian maximum contact pressure. Surface roughness was Ra=0.4µm for both materials.
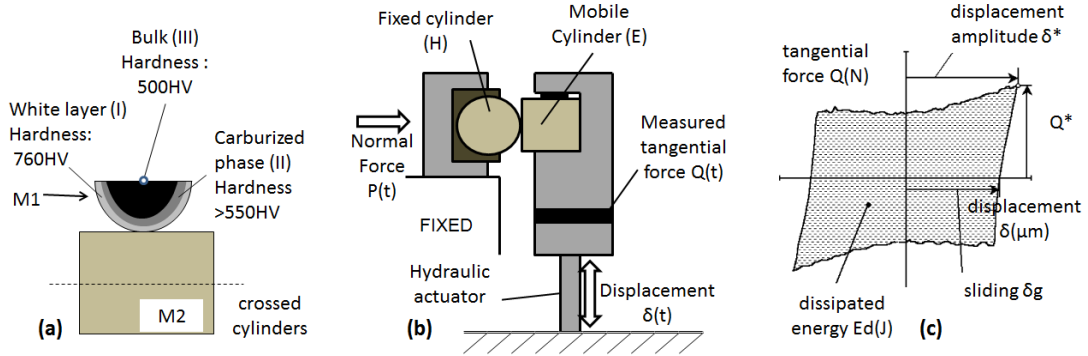
Figure 1: (a) Contact configuration (crossed cylinders); (b) Fretting setup; (c) Fretting cycle analysis.

2.2 Test System

Figure 1b shows a diagram of the fretting wear test. An MTS hydraulic tension-compression machine regulated displacement between cylinders (further details of this setup and experimental method used can be found in (Fouvry, 1996)). During the test, normal force P was kept constant by a feedback system, and the cyclic sinusoidal displacement $\delta*$ was applied to generate an alternating tangential load $Q*$ on the contact. All tests were performed with a constant frequency of 3 Hz, at room temperature. This enabled the fretting loop Q-δ to be plotted for chosen cycles (Figure 1c). During tests, displacement amplitude was fixed between $\pm100\mu m$ and $\pm1000\mu m$, leading to two generalized slip regimes: gross slip in fretting, and reciprocating. The first tests were performed with $\pm300\mu m$ displacement and different numbers of cycles, and the second with different displacement amplitudes $\delta*$ and numbers of cycles N. Because of system stiffness, the sliding amplitude δg was not always the same for a given displacement amplitude. For each test, slip was generalized in the interface, and the ratio $Q*/P$ was supposed to be constant for any displacement amplitude.

The ratio $Q*/P$ was then defined as the coefficient of friction μ, and the dissipated energy Ed during the fretting cycle was given by the area of the corresponding hysteresis cycle (see Figure 1c). The accumulated friction energy was determined by summing friction loop energy over the whole test duration:

$$\sum Ed = \sum Ed_{(i)} \approx 4.N.\delta g.\mu.P \qquad (1)$$

Wear volume (V) after testing was measured on a 3D scan. Wear rate was established from wear volume versus accumulated friction energy (Archard, 1953). Figure 2a compares evolution of wear volume in M1 and M2 specimens versus accumulated friction energy. Wear volume evolution was linear in M2 but showed a bilinear tendency in M1, linked to the structure of the M1 interface (Figure 1a): wears initially involved the brittle white
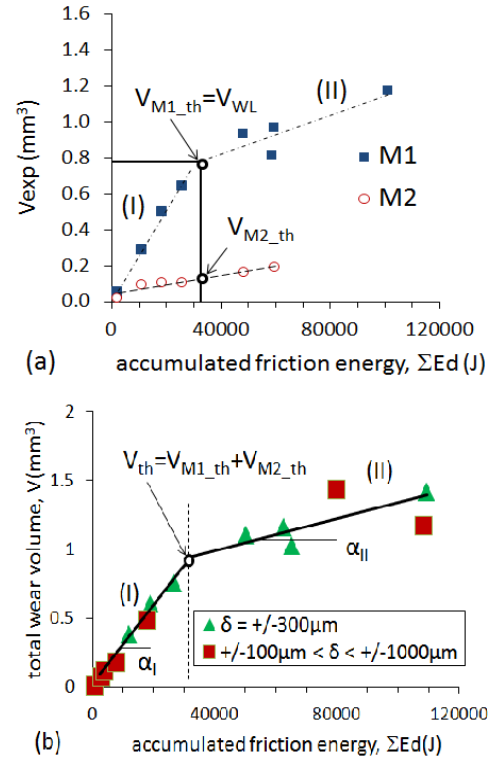

Figure 2: (a) Evolution of wear volume VM1 and VM2; (b) Total wear volume evolution (V=VM1 + VM2) versus accumulated friction energy (Vth; αI and αII are defined from the δ=$\pm300\mu m$ experiments).

layer of M1 (WL) before reaching the subsurface carburized layer (CL), the wear rate was lower. It is noteworthy that, while the wear rate in the counter-body was equivalent to that of the $M1_{CL}$ layer (II), that of the M1 top WL layer (I) displayed significantly (approx. 10-fold) higher wear kinetics.

Total wear volume $V = V_{M1} + V_{M2}$ is related to total accumulated friction energy (Figure 2b). Considering the difference between the top WL response and sub-carburized layer, a bilinear energy wear model can be introduced as follows:

- If $V < V_{th}$, the interface involves the $M1_{WL}$ domain, and $V_{Ed} = \alpha_I . \Sigma Ed$
- If $V > V_{th}$, all the $M1_{WL}$ phase has been worn out and the interface involves only the $M1_{CL}$ sub-carburized layer, and $V_{Ed} = \alpha_{II} . (\Sigma Ed - Ed_{th}) + V_{th}$

where $Ed_{th} = V_{th}/\alpha_I$, V_{th} is the threshold wear volume related to M1 white layer elimination (V_{WL}) plus associated M2 wear. V_{WL} can be expressed as a function of the contact area A_f and the white layer thickness (h_{WL}) (i.e., $V_{WL} = h_{WL} . Af$), where α_I is the energy wear rate of the $M2/M1_{WL}$ interface, and α_{II} is the energy wear rate of the $M2/M1_{CL}$ interface.

Using this very simple physical model involving only 3 material parameters (V_{th}, α_I, and α_{II}), it is possible to express the total wear kinetics of the interface. The theoretical description is compared with the experimental results in Figure 3. The results related to $\delta^* = +/-300\mu m$ fretting sliding are also compared with other results for fretting and large reciprocating sliding conditions. The regression coefficient is about $R^2 = 0.9045$, which confirms the
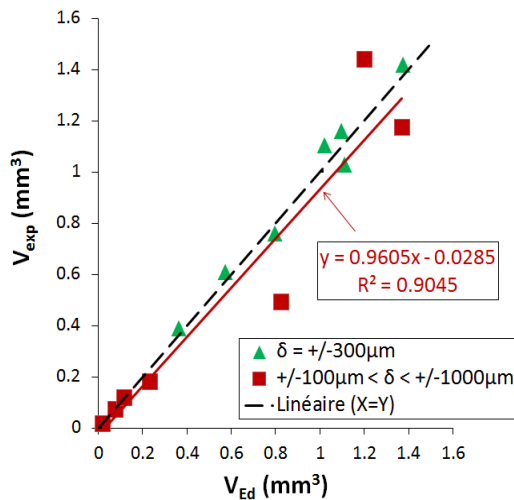
stability of the energy approach to formalizing wear rate even for a complex interface like that investigated here.

3   MODELING   WEAR EVOLUTION

This wear behavior could not be predicted or expected initially, because of the bi-linear phenomenon, for which a static Neural Network was used to estimate wear evolution as a function of dissipated energy Ed with respect to mechanical variables and environmental conditions (Figure 4). A dynamic Neural Network could not be used because of the poor database. We propose 3 models with different key input parameters. The input data are P, δg, μ and N for the first network (Model_A), only Ed for the second (Model_B) and a combination of all 5 parameters for the third (Model_C). Model_A and Model_B could be expected to give the same results, as Ed can be approximated by the inputs of Model_A as shown in Eq.1.
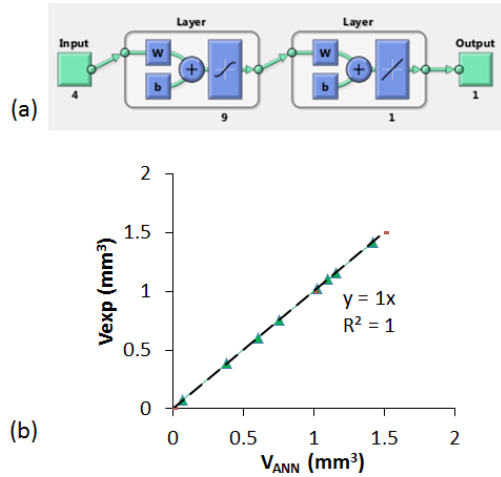

Figure 4: (a) Schematic description of the network structure; (b) Network training results.

The structure adopted was a two layer network with 9 neurons in the hidden layer and 1 in the output layer (Figure 4a). For the input layer, the transfer function was a sigmoidal tangent (*tansig*), and for the last layer a linear function (*purelin*).

The three models were assessed by comparing experimental and predicted wear volume. The experiments performed with ±300µm displacement amplitude with different numbers of cycles constituted training data, and the other experiments

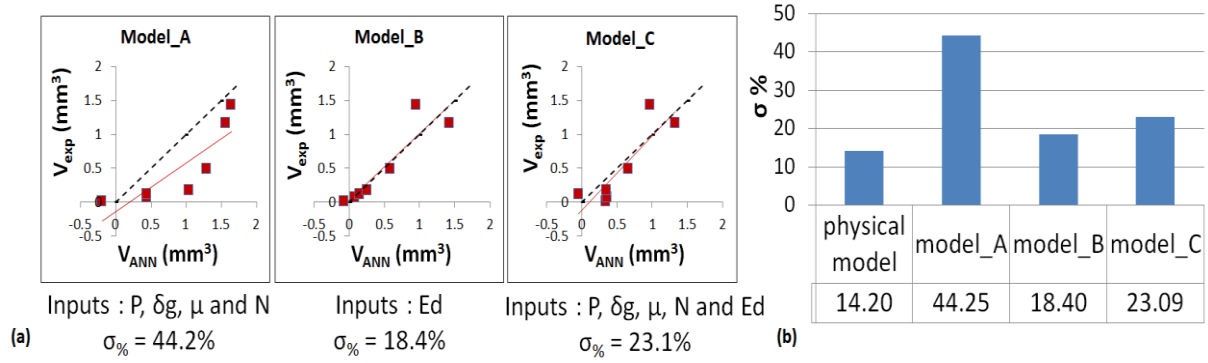Figure 3: Comparison of experimental (Vexp) and theoretical (VEd) wear volume

Figure 5: (a) Test results of the three Neural Networks; (b) Variance results of the physical model and the three ANN models

(±100µm to ±1,000µm with different numbers of cycles) represent the test data. Simulation could be expected to be difficult, as the network could not be trained on the variable δg. Figure 4b, however, shows excellent network training, with R^2=1 for each model. To compare the models, the percentage square root of normalized variance was defined as follows:

$$\sigma_\% = \frac{\sqrt{\frac{\sum_{i=1}^{Z}(Xi - Ui)^2}{Z}}}{V_{max}} * 100 \tag{2}$$

where Xi is the experimental wear data, Ui the predicted wear data, Z the number of samples, and V_{max} the maximum experimental wear volume.

4   RESULTS AND DISCUSSION

The variance σ of the physical energy wear model was about 14.2 % (Figure 3). All simulated wear volume results for the 3 models are presented in Figure 5a.
Model_A was unable to predict wear volume, as the correlation was poor (σ = 44.2%). Model_B had only Ed input, the key parameter in this study; correlation was excellent (σ = 18.4%) and only 4.2% different from the experimental correlation. The input variables used in Model_A could be used to calculate the dissipated energy Ed (Eq.1), whereas the neural network could not achieve this internally to give a good estimate of wear volume, probably due to the small amount of data available for network training. Model_B was more reliable than Model_A. In Model_C, all the parameters are considered as inputs; the linear regression R^2 was better than in the other models, but the dispersion was greater (σ = 23.1%); wear prediction for low accumulated dissipated energy was poorer than in Model_A, but for higher energy the results were similar to those of Model_B.

5   CONCLUSION

A static Artificial Neural Network was built and validated for variable fretting and reciprocating conditions. In-situ wear volume measurement enabled a model describing wear behavior to be created, providing reliable simulation of wear. The ANN model assessed wear volume almost as well as the physical model (Figure 5b) in spite of the small amount of experimental data. At this point in the study, it is difficult to choose between Model_B and Model_C: one had a better correlation factor, whereas the other had less dispersion. Model_B provided better wear prediction for low accumulated dissipated energy. However, this issue needs more investigation. Another crucial issue is the size of the database used for the training and the test; this is a recurrent problem in many industrial applications, where the amount of data is insufficient for effective parameterization of standard neural structures. In such situations, one possible approach is to consider the hidden layer as "simply" a projection operator, given which learning could be performed on the output layer alone. These aspects (projection operator and output learning) need to be investigated more precisely to optimize estimation of wear volume.

REFERENCES

Anand Kumar S., Ganesh Sundara Raman S., Sankara Narayanan T.S.N., Gnanamoorthy R., 2013. Materials and Design. *Prediction of fretting wear behavior of surface mechanical attrition treated Ti–6Al–4V using artificial neural network*. Volume 49, Pages 992–999.

Archard J. F., 1953, Journal of Applied Physics. *Contact and Rubbing of Flat Surfaces*. Volume 24(8), Pages 981-988.

Fouvry S., Kapsa Ph., Vincent L., 1996. Wear. *Quantification of fretting damage.* Volume 200, Pages 186-205.

Genel K., Kurnaz S.C., Durman M., 2003, Materials Science and Engineering. *Modeling of tribological properties of alumina fiber reinforced zinc–aluminum composites using artificial neural network*. Volume A363, Pages203–210.

Kolodziejczyk T., Toscano R., Fouvry S., Morales-Espejel G., 2010. Wear. *Artificial intelligence as efficient technique for ball bearing fretting wear damage prediction*. Volume 268, Issues 1–2, Pages 309-315.

Sahraoui T., Guessasma S., Fenineche N.E., Montavon G., Coddet C., 2004. Materials Letters. *Friction and wear behaviour prediction of HVOF coatings and electroplated hard chromium using neural computation.* Volume 48, Pages 654– 660.

Zhang Z., Barkoula N.-M., Karger-Kocsis J., Friedrich K., 2003. Wear. *Artificial neural network predictions on erosive wear of polymers*. Volume 255, Pages708–713.